Acta Biomaterialia 64 (2017) 269–278

Contents lists available at ScienceDirect

Acta Biomaterialia

journal homepage: www.elsevier.com/locate/actabiomat

Full length article

Influence of dynamic compressive loading on the *in vitro* degradation behavior of pure PLA and Mg/PLA composite

Xuan Li [a,b,c], Chenxi Qi [a,b], Linyuan Han [a,b], Chenglin Chu [a,b,*], Jing Bai [a,b], Chao Guo [a,b], Feng Xue [a,b], Baolong Shen [a,b], Paul K. Chu [c,*]

[a] School of Materials Science and Engineering, Southeast University, Nanjing 211189, China
[b] Jiangsu Key Laboratory for Advanced Metallic Materials, Southeast University, Nanjing 211189, China
[c] Department of Physics and Materials Science, City University of Hong Kong, Tat Chee Avenue, Kowloon, Hong Kong, China

ARTICLE INFO

Article history:
Received 20 April 2017
Received in revised form 18 July 2017
Accepted 3 August 2017
Available online 4 August 2017

Keywords:
Dynamic compressive loading
Mg/PLA
Internal fixation implants
Load frequency
Degradation kinetics

ABSTRACT

The effects of dynamic compressive loading on the *in vitro* degradation behavior of pure poly-lactic acid (PLA) and PLA-based composite unidirectionally reinforced with micro-arc oxidized magnesium alloy wires (Mg/PLA) are investigated. Dynamic compressive loading is shown to accelerate degradation of pure PLA and Mg/PLA. As the applied stress is increased from 0.1 MPa to 0.9 MPa or frequency from 0.5 Hz to 2.5 Hz, the overall degradation rate goes up. After immersion for 21 days at 0.9 MPa and 2.5 Hz, the bending strength retention of the composite and pure PLA is 60.1% and 50%, respectively. Dynamic loading enhances diffusion of small acidic molecules resulting in significant pH decrease in the immersion solution. The synergistic reaction between magnesium alloy wires and PLA in the composite is further clarified by electrochemical tests. The degradation behavior of the pure PLA and PLA matrix in the composite under dynamic conditions obey the first order degradation kinetics and a numerical model is postulated to elucidate the relationship of the bending strength, stress, frequency, and immersion time under dynamic conditions.

Statement of significance

We systematically study the influence of dynamic loading on the degradation behavior of pure PLA and Mg/PLA. Dynamic compressive loading is shown to accelerate degradation of pure PLA and Mg/PLA. The synergistic reaction between magnesium alloy wires and PLA in the composite is firstly clarified by electrochemical tests. The degradation behavior of the pure PLA and PLA matrix in the composite under dynamic conditions obey the first order degradation kinetics. Then, a numerical model is postulated to elucidate the relationship of the bending strength, stress, frequency, and immersion time under dynamic conditions.

1. Introduction

Bone fracture fixation devices are widely used to assist bone regeneration in patients [1,2]. The obvious technique is rigid fixation [2,3] in which the fracture is totally stabilized to avoid movement but it has been shown that it may result in implant loosening of the implant and healing delay [4,5]. On the other hand, flexible internal fixation in which some mobility at the fracture gap is allowed [6,7] can enhance the formation of callus that bridges fractured bones and consequently promote bone healing [6,7]. In fact, the healing efficacy is strongly related to the fracture gap and a wide gap may adversely affect healing [8,9]. Therefore, the external compressive load applied to the implants during motion cannot be very large.

Internal fixation implants such as screws and plates can be removed after fracture healing and so biodegradable implants are being developed to obviate the need for a second operation to remove the implants. Poly-lactic acid (PLA) is quite biocompatible and used in biodegradable implants [10,11]. Commercial PLA-based materials have been currently used as fixation-devices such as screws [12], pins [13] and darts [14] in reconstructive surgeries for anterior cruciate ligament reconstruction, soft tissue fixation,

* Corresponding authors at: School of Materials Science and Engineering, Southeast University, Nanjing 211189, China (C. Chu).
E-mail addresses: clchu@seu.edu.cn (C. Chu), paul.chu@cityu.edu.hk (P.K. Chu).

https://doi.org/10.1016/j.actbio.2017.08.004
1742-7061/

hyaline cartilage fixation, and pediatric craniotomy fixation [15]. However, the mechanical properties of PLA are still inferior and the acidic degradation products may induce inflammation [16,17]. In opposition to PLA, magnesium alloys emerge higher mechanical strength, stiffness and the beneficial role promoting osteogenesis [18]. However, the rapid degradation and the pH increase associated with the degradation limit the bioapplications of Mg alloys. Therefore, many efforts [18] are devoted to slow down the degradation rate of Mg alloys *in vivo* including surface treatments, alloying and amorphization.

Previously, the composite composed of poly (a-hydroxy acids) and Mg alloys is proposed to overcome the aforementioned drawbacks [19–22]. In this kind composite, Mg alloy based fillers (Mg fillers) such as Mg particles [21,22] or Mg alloy fibers [23] are incorporated into biodegradable polymers and the composite shows the following advantages [20–23]: (i) the mechanical properties of polymer matrix could be improved with the reinforcing of Mg fillers; (ii) the degradation of Mg fillers could be mitigated with the protection of the polymer matrix; (iii) pH value of the surround environment could be stabilized during immersion; (iv) addition of Mg fillers may promote the biomineralization and cell adhesion. Very recently, we used micro-arc oxidized magnesium alloy wires (MAWs) as the fillers to reinforce PLA [24,25]. Our studies show the composite has desirable mechanical and degradation properties [26,27]. This kind composite is promising for bone fixation implants. *In vivo*, the mechanical properties of implants are desired to match those of the surround tissues. Since the implants often experience compression loading in service which may significantly influence the mechanical behaviors of the implants, it is crucial to understand the effects of compression loading on their degradation behavior. In fact, it has been demonstrated that bone growth and healing are related to the mechanical loads [28–30]. Normally, dynamic loading promotes bone formation which can be further improved by increasing the loading magnitude and frequency [31,32]. In this study, the effects of these two factors and degradation behavior of pure PLA and Mg/PLA composite under dynamic compressive loading are investigated.

2. Materials and methods

2.1. Materials

The PLA particles (density: 1.24 g/cm^3, glass transition temperature: 65 °C, melting temperature: 168 °C, crystallinity: 38%) were purchased from Natureworks LLC. Magnesium alloys wires (MAWs) with a diameter of 0.3 mm (AZ31: 96% Mg, 3% Al and 1% Zn by weight) were fabricated by continuous smelting, casting, hot extrusion, wet drawing, and annealing. The MAWs were micro-arc oxidized on the WHD-30 type MAO equipment [33]. The pure PLA and Mg/PLA plates were prepared using a stack-heat-compressing process [27] and the volume fraction of MAWs in the composite was 10 vol%. After the fabrication, the crystallinity of pure PLA and PLA matrix in the composite respectively increased to about 49% and 52%, while the melting temperature slightly increased to 171 °C. The viscosity average molecular weight of pure PLA and PLA matrix in the composite is controlled to between 72,000 and 74,000 g/mol. This slight difference may suggest the presence of MAWs does not significantly influence the crystallinity and viscosity average molecular weight of the PLA matrix, agreeing with the reported results that Mg particles do not induce crystal nucleation of PLLA during cooling from the melt [22].

2.2. Dynamic immersion tests

The apparatus used in the dynamic immersion tests is shown in Fig. 1 and the dynamic compressive load was applied through a double-acting air cylinder. The loading magnitude was regulated by the pressure of the gas flow and the frequency was modified by a switch-on clock. The sample was put in honeycombed polytetrafluoroethylene connected to the bottom of a polytetrafluoroethylene plate through threaded joints. The dimensions of the specimen were 50 mm × 12 mm × 2 mm. The Kirkland's biocorrosion media (KBM) [34] with a pH 7.4 at 37 °C was used as the immersion fluid and the volume was 500 ml. The fluid was changed every day and prior to changing, the pH was measured. Normally, the strain of bones under different activities is about 400×10^{-6}–2000×10^{-6} [35] and the dynamic frequency is 1–3 Hz [36]. After the surgical procedure, the fracture tissues are restricted from applying large loadings and the applied strain should be very small. It is reported that intramembranous bone formation was found for small hydrostatic pressure (<0.15 MPa), while hydrostatic pressure more than 0.15 MPa could stimulate endochondral ossification [37]. Then, the stress loads applied to the samples were predetermined to be 0 MPa (static), 0.1 MPa, 0.3 MPa, and 0.9 MPa at frequencies of 0.5 Hz, 1 Hz, and 2.5 Hz. The immersion durations were 7 days, 10 days, 15 days, and 21 days.

The viscosity average molecular weight (M_v) of PLA was calculated by the Mark-Houwink-Sakurada formula [38]. The mass loss ratio (ω) was calculated using the following equation:

$$\omega = ((m_0 - m_t)/m_0) \times 100\%, \quad (1)$$

where m_0 is the initial mass and m_t is the final mass of the sample after immersion after drying for 48 h in an oven at 37 °C.

2.3. Electrochemical tests

Electrochemical impedance spectroscopy (EIS) was conducted under static conditions using a CHI604 potentiostat workstation (Shanghai Chenhua Instrument, China). The frequencies were scanned from 100 kHz to 0.1 Hz and the amplitude was 10 mV. Prior to the tests, one end of the sample was dissolved in chloroform and the exposed MAW was connected to a wire. During the test, the other end of the composite with a length of 30 mm was immersed in the KBM solution at 37 °C. Two MAWs in the composite at different locations were measured: one near the surface of the composite (the outer MAW) and the other is in the middle of the composite (the inner MAW). The reference and counter electrodes were, respectively, a saturated calomel electrode (SCE) and Pt electrode and the MAW was the working electrode.

2.4. Mechanical tests and microstructural characterization

The three-point bending tests were conducted according to the standard ASTMD790-2010 on the CMT4503 electronic universal testing machine at room temperature at a crosshead speed of 2 mm/min. The bending span was 32 mm. Scanning electron microscopy (SEM) was performed on the Philips XL30 FEG at an accelerating voltage of 20–25 kV and the elemental composition was determined by energy-dispersive X-ray spectrometry (EDS). The specimens were mounted on a stub and sputter-deposited with a thin platinum layer in argon.

2.5. Statistical analysis

The data was statistically analyzed and presented as averages of three measurements together with standard deviations and least-square fits were applied to the curves when possible. The coefficient of determination (R^2) was used to evaluate the fitting results. The statistical software Origin (OriginLab Corporation, Northampton, USA) was used in the data analysis.

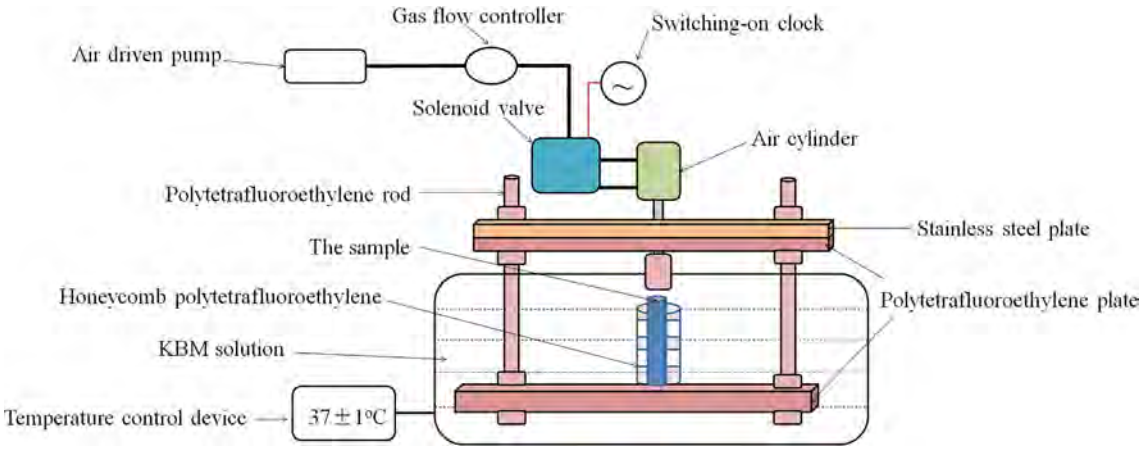

Fig. 1. Schematic illustration of the apparatus used in the dynamic test.

3. Results

3.1. Degradation behavior of pure PLA under dynamic conditions

The pH changes in the solutions during the immersion of pure PLA under static condition (no load) and dynamic conditions at 1 Hz at different magnitudes are displayed in Fig. 2(a). The pH values decrease significantly under dynamic conditions compared to static condition. During the first 7 days, the pH gradually decreases with increasing stress level. At 0.9 MPa, an apparent pH decrease is observed after 15 days as shown in Fig. 2(a). The ω changes are shown in Fig. 2(b). ω increases with increasing loads and is about 1% at 0.9 MPa after 21 days. The M_v changes in the PLA are presented in Fig. 2(c). M_v decreases with immersion time and a higher stress level reduces M_v more. S_b also changes during immersion as shown in Fig. 2(d). The original S_b of pure PLA is about 110 MPa and after immersion for 21 days, it decreases to about 90 MPa, 82 MPa, 74 MPa and 66 MPa at 0 MPa (static), 0.1 MPa, 0.3 MPa, and 0.9 MPa, respectively.

Fig. 3 shows the degradation behavior of pure PLA at 0.9 MPa at different loading frequencies. The pH values at 1 Hz and 2.5 Hz are less than those at 0.5 Hz during immersion, as shown in Fig. 3(a).

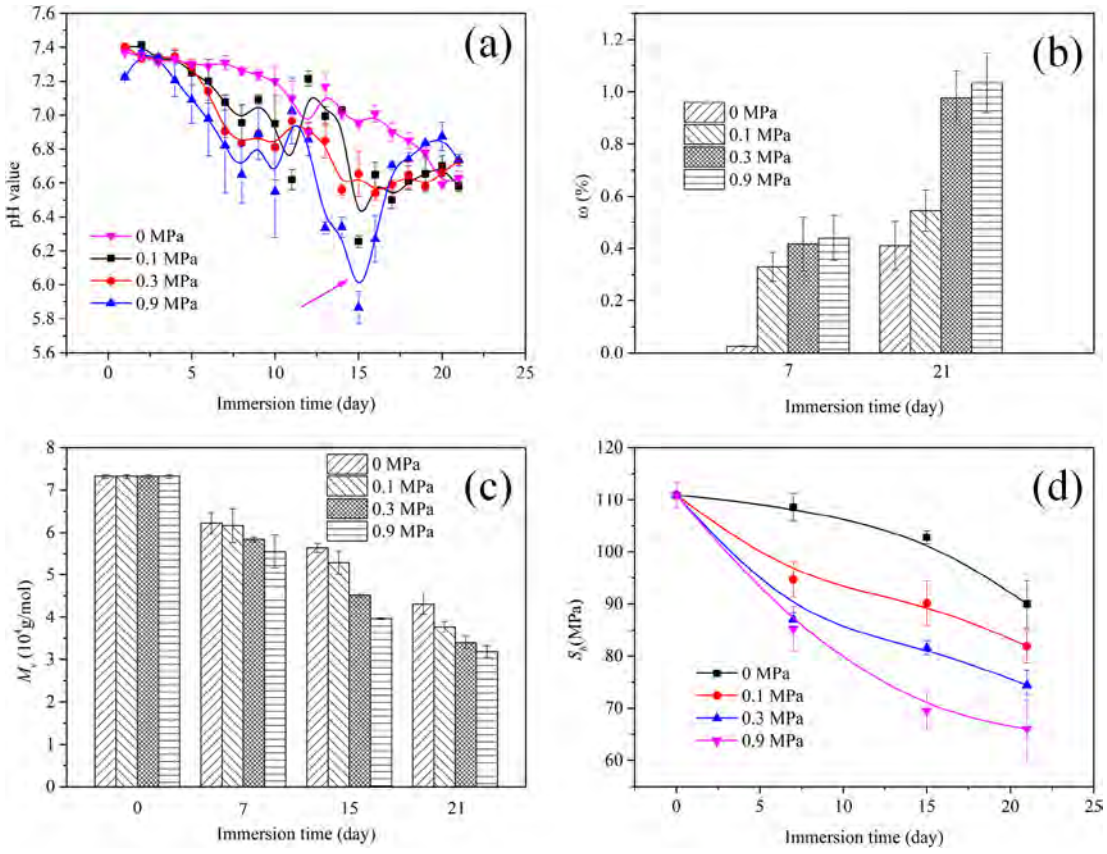

Fig. 2. Degradation behavior of pure PLA under static and dynamic conditions at 1 Hz and different stress levels versus immersion time: (a) pH variation; (b) ω variation; (c) M_v variation; (d) S_b variation.

Significant pH decrease is observed after 7 and 15 days at 2.5 Hz and 1 Hz. ω increases but M_v and S_b decrease with increasing load frequencies. After immersion for 21 days, M_v of PLA is 49%, 44% and 37% of the initial value, whereas S_b exhibits 0.27, 0.4 and 0.5 times reduction at 0.5 Hz, 1 Hz, and 2.5 Hz, respectively. A large loading frequency is observed to enhance degradation of pure PLA.

3.2. Degradation behavior of Mg/PLA under dynamic conditions

The degradation behavior of Mg/PLA under static and dynamic conditions at 1 Hz and different stress levels are shown in Fig. 4. The pH values decrease under dynamic conditions. As the stress increases, ω increases and a value of 1.9% is observed at 0.9 MPa after 21 days and it is larger than that of the pure PLA. Similar to pure PLA, M_v and S_b decrease with stress. After 21 days, S_b is 112 MPa, 99 MPa, 95 MPa, and 91 MPa at 0 MPa (static), 0.1 MPa, 0.3 MPa, and 0.9 MPa, respectively.

Fig. 5 shows the effects of the load frequency on the degradation behavior of Mg/PLA. The pH at 1 Hz and 2.5 Hz is smaller than that at 0.5 Hz. After 21 days, ω at 2.5 Hz is 2.8% that is nearly 2.5 times that at 0.5 Hz. A larger frequency also decreases M_v and S_b. After 21 days, M_v is about 4.29×10^4 g/mol, 3.66×10^4 g/mol, and 3.34×10^4 g/mol and S_b is 104 MPa, 90 MPa, and 82 MPa at 0.5 Hz, 1 Hz, and 2.5 Hz, respectively.

3.3. Surface morphology

Fig. 6 shows the surface morphology of the MAWs in the composite after dissolving the PLA matrix in chloroform and immersion for 21 days immersion at 0.9 MPa and different load frequencies. At 0.5 Hz, the surface coating is integrated but micro cracks are observed. However, at 1 Hz and 2.5 Hz, the coatings exhibit critical breakage and white precipitate appears. EDS shows that the precipitation formed at 2.5 Hz contains Ca and P indicating that a large loading frequency promotes precipitation of the Ca-P phase on the surface of the MAWs in the composite.

3.4. Electrochemical tests

Electrochemical tests are conducted to determine the degradation behavior of MAWs in the composite. Fig. 7(a) and (b) show the Nyquist plots of the outer and inner MAWs in the composite after 4 days. The inner MAW shows a larger capacitance loop than the outer one. The spectra are fitted with the equivalent circuit model in Fig. 7(c) and a constant phase element (CPE) instead of an ideal capacitor is used to compensate for the surface inhomogeneity [39]. R_{sol} is the resistance of the solution and the evolution of polarization resistance (R_p) of the two MAWs versus immersion time is shown in Fig. 7(d). After 1 day, R_p of the inner MAW ($R_{p\text{-inner}}$) is larger than that of the outer MAW ($R_{p\text{-outer}}$), indicating that a thicker PLA matrix surrounds the inner MAW. After 5 days, $R_{p\text{-inner}}$ is about 1300 $\Omega\,cm^2$ whereas it is only about 80 $\Omega{\cdot}cm^2$ for $R_{p\text{-outer}}$. As the immersion time is increased to 7 days, $R_{p\text{-inner}}$ decreases to 400 $\Omega{\cdot}cm^2$ and $R_{p\text{-outer}}$ is constant at about 80 $\Omega{\cdot}cm^2$. Thereafter, $R_{p\text{-outer}}$ increases gradually versus immersion time, whereas $R_{p\text{-inner}}$ increases initially and then decreases gradually.

4. Discussion

4.1. Degradation characteristics of pure PLA and Mg/PLA

The bending strength is an important property of biomedical implants. The S_b retention observed from the samples under static and dynamic conditions after immersion for 21 days is shown in

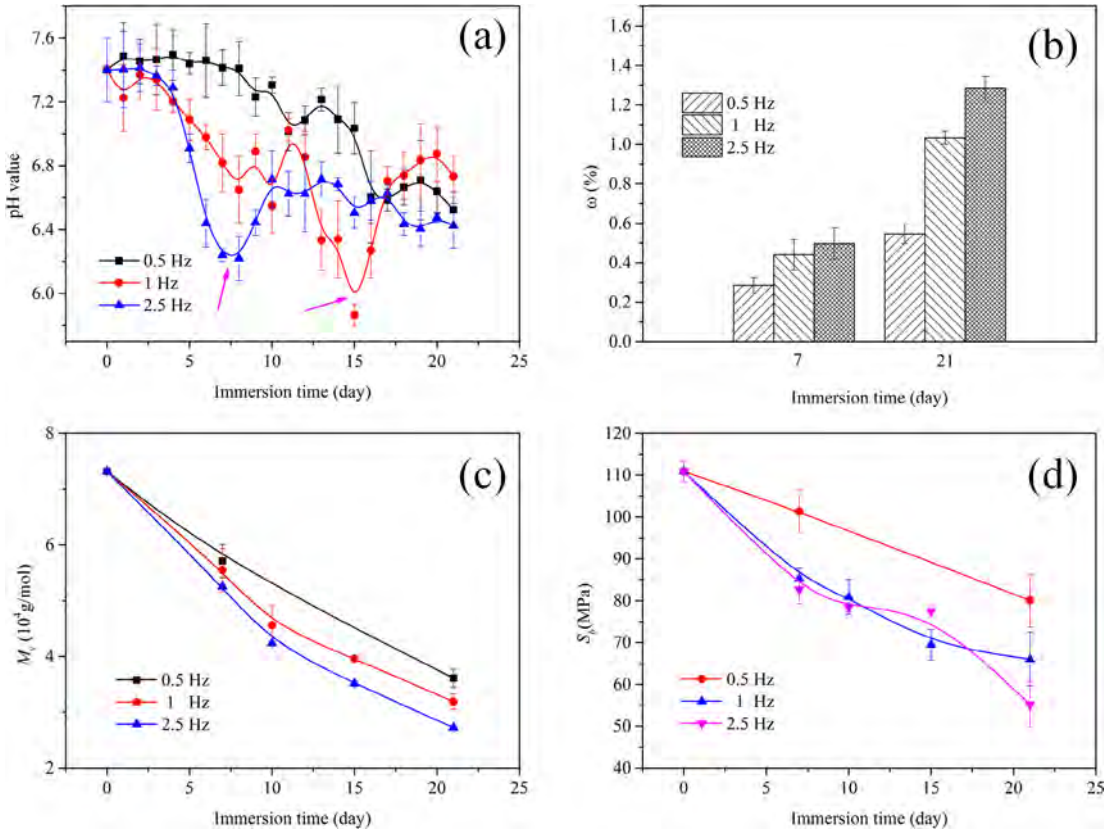

Fig. 3. Degradation behavior of pure PLA at 0.9 MPa and different frequencies versus immersion time: (a) pH variation; (b) ω variation; (c) M_v variation; (d) S_b variation.

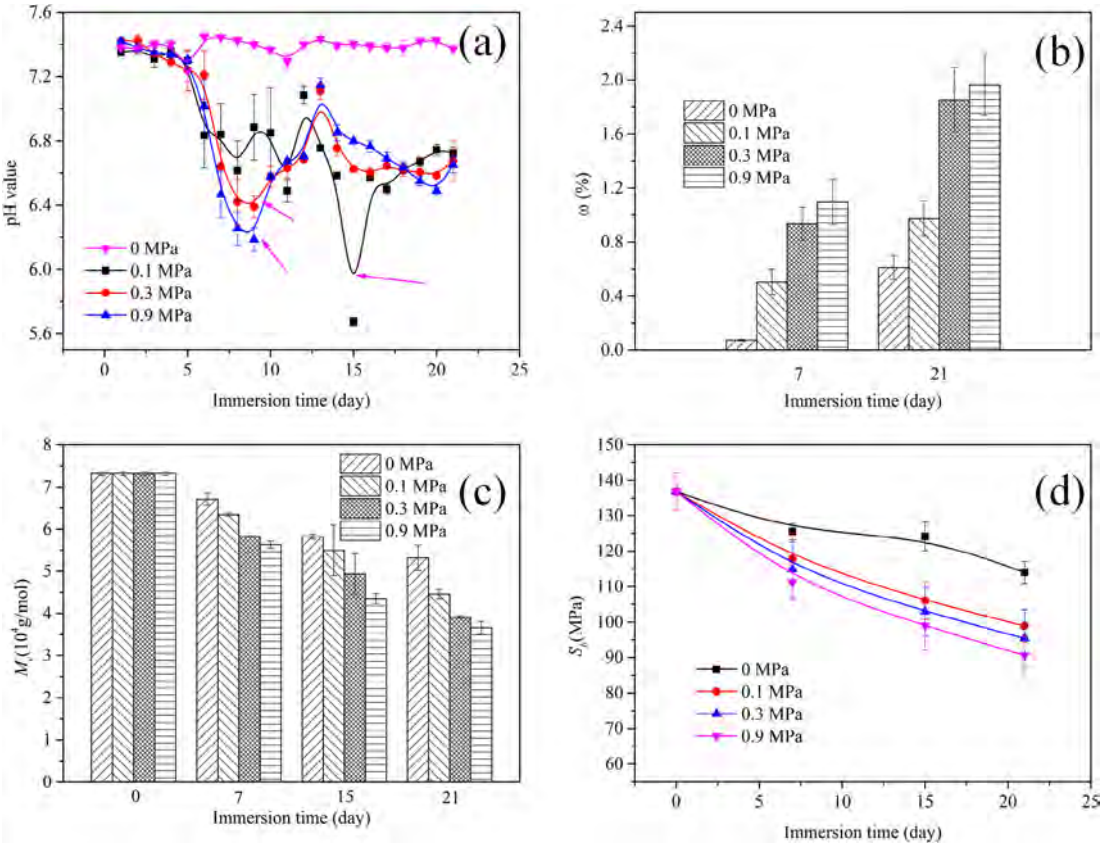

Fig. 4. Degradation behavior of Mg/PLA under static and dynamic conditions at 1 Hz and different stress levels versus immersion time: (a) pH variation; (b) ω variation; (c) M_v variation; (d) S_b variation.

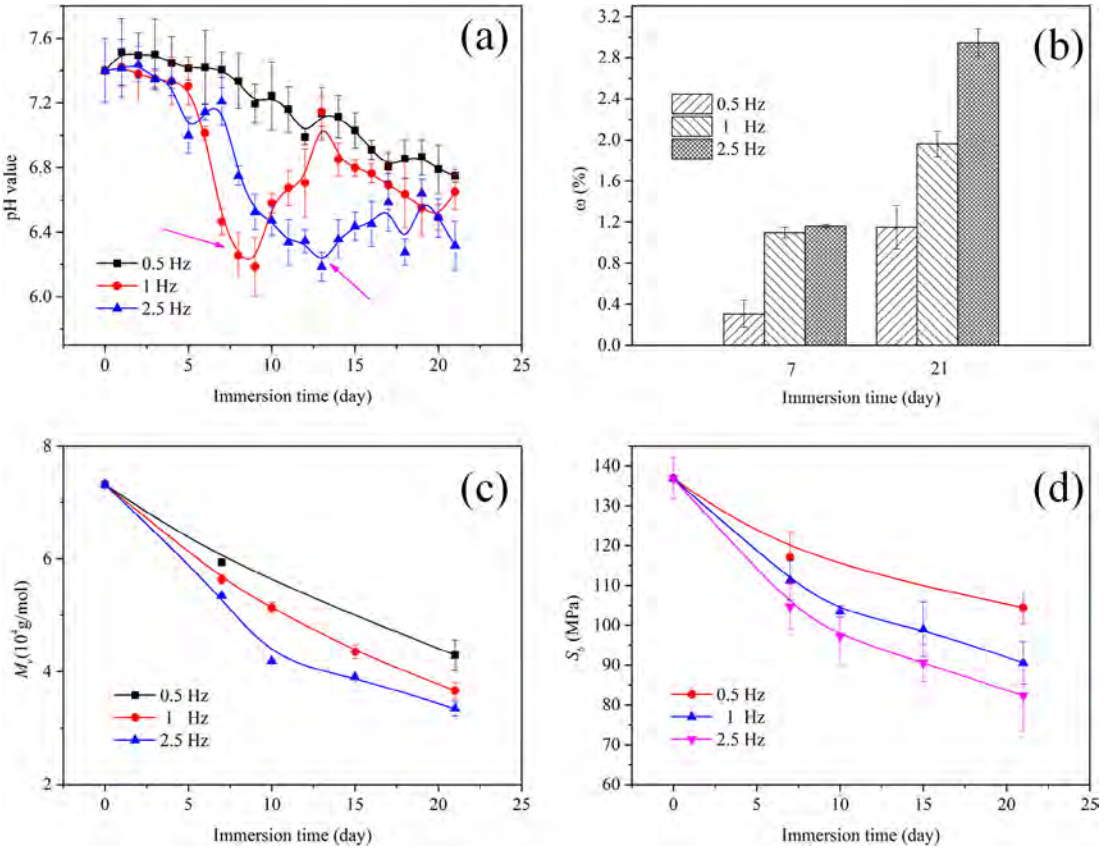

Fig. 5. Degradation behaviors of Mg/PLA at 0.9 MPa at different frequencies versus immersion time: (a) pH variation; (b) ω variation; (c) M_v variation; (d) S_b variation.

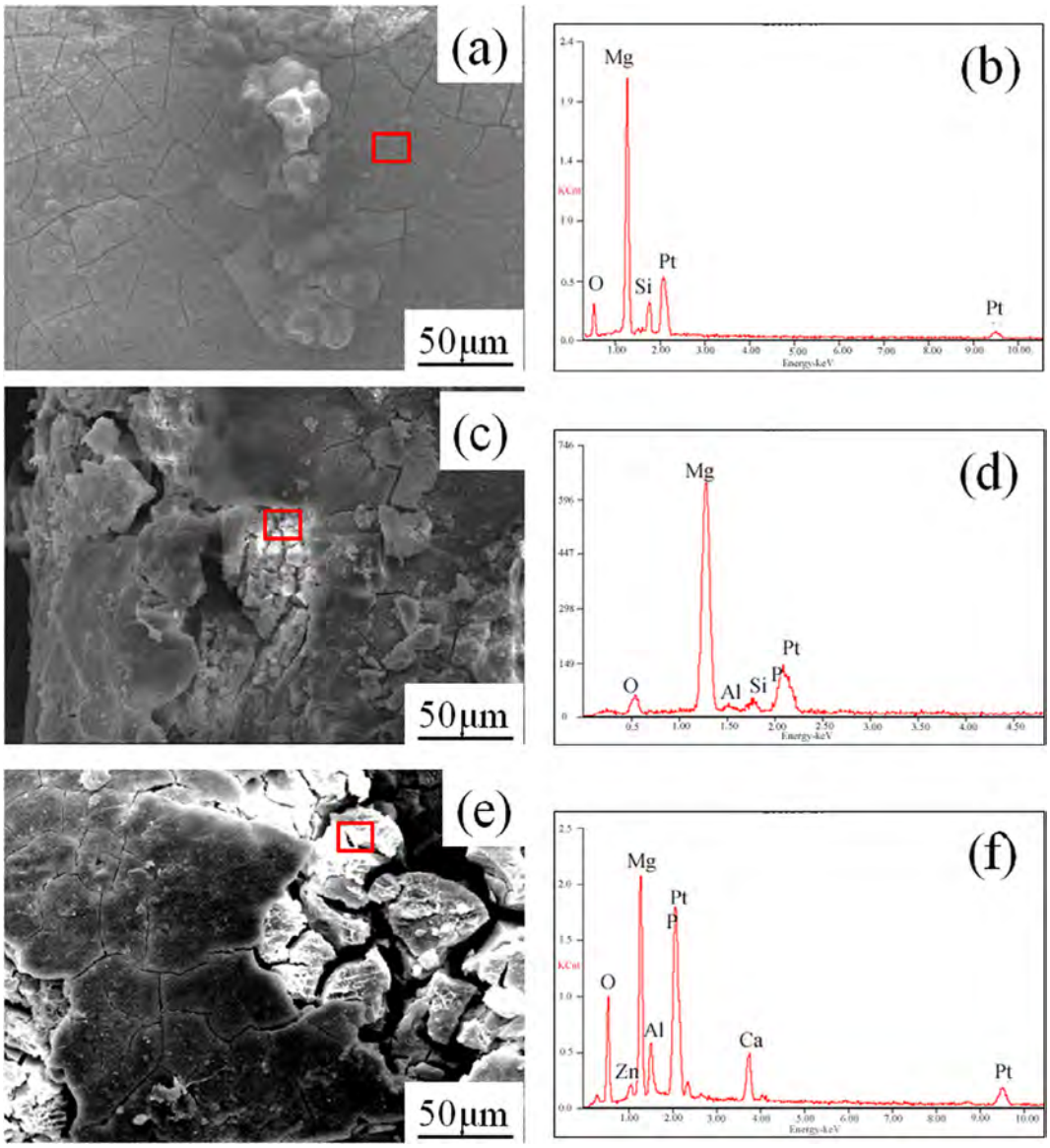

Fig. 6. Surface morphology of the MAWs in Mg/PLA after immersion for 21 days at 0.9 MPa and different loading frequencies: (a) 0.5 Hz; (b) EDS spectrum for 0.5 Hz; (c) 1 Hz; (d) EDS spectrum for 1 Hz; (e) 2.5 Hz; (f) EDS spectrum for 2.5 Hz.

Table 1. Overall, Mg/PLA has better strength retention ability than pure PLA under dynamic conditions, especially at high frequencies. Decomposition of Mg release Mg ions which neutralize acidic products derived from the degradation of PLA [23,40] as confirmed by the maintained pH during the immersion of the Mg/PLA under the static condition. However, neutralization is not apparent under dynamic conditions for the composite, although the PLA matrix in the composite has a smaller degradation rate than pure PLA. According to the evolution of R_p of the inner MAW and the pH change in the solution, initial degradation of the composite probably comprises into four stages as shown in Fig. 7(d):

a) The first stage is diffusion of water molecules and degradation of the outer MAWs. In this stage, MgO or Mg^{2+} reacts with carboxylic acid from the PLA [26,41,42] resulting in reduction in the solubility of PLA, retardation of degradation of PLA, and apparent $R_{p\text{-inner}}$ increase.
b) The second stage is accumulation of acidic ions inside the composite (or pure PLA) reducing $R_{p\text{-inner}}$. This process is corroborated by the pH decrease for pure PLA and the composite under dynamic conditions. Dynamic loading enhances the fluid flow in and out of the sample to promote migration of the small acidic molecules to the solution [43]. In the composite, the interface between the MAWs and matrix provides an additional diffusion pathway.
c) The third stage involves neutralization. The acidic environment in the composite accelerates degradation of the inner MAWs. In this process, acidic ions are consumed and $R_{p\text{-inner}}$ increases.
d) The fourth stage involves the reaction of the degradation products from the MAWs and PLA. Acidic degradation of PLA promotes degradation of MAWs, mitigates pH decrease, and leads to gradual degradation of the composite.

4.2. Effects of dynamic loading

Compression loads such as those expected for bone healing can alter the mechanical properties of the implants [44,45]. Our previous experiments show that S_b retention of the unstressed pure PLA and Mg/PLA after immersion for 30 days is 74% and 78% and

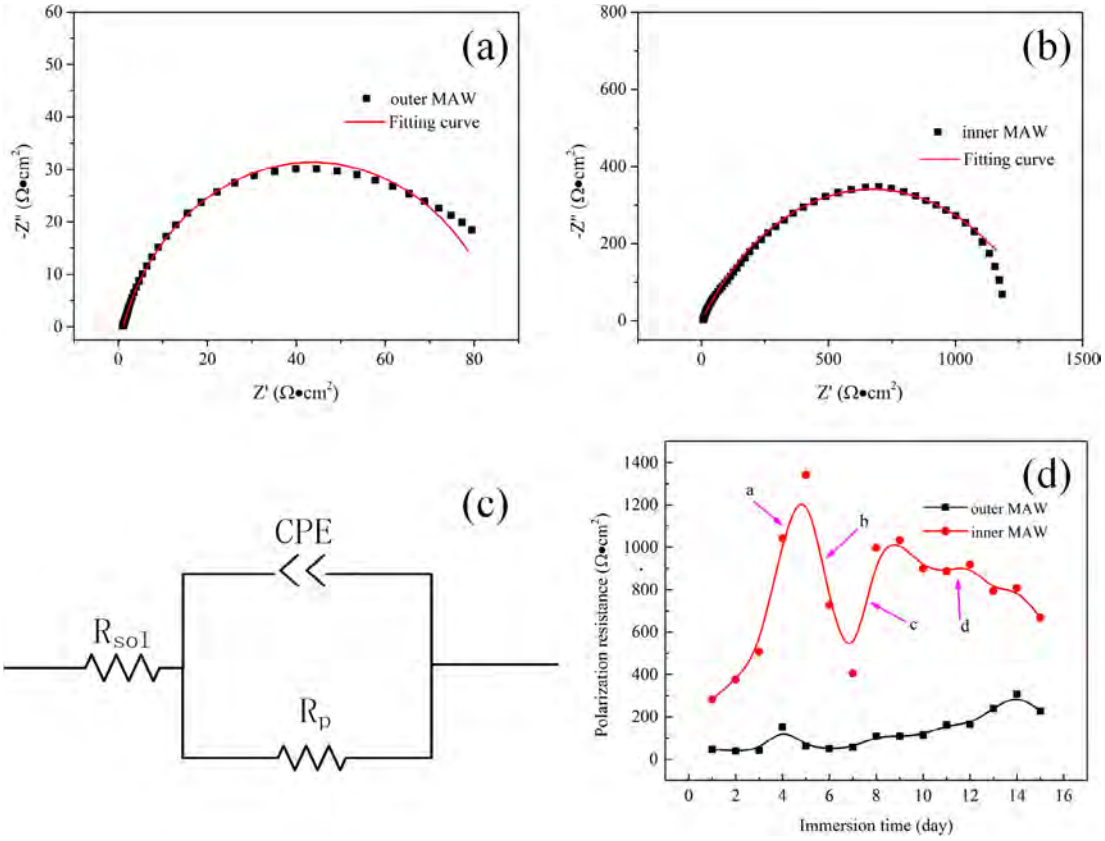

Fig. 7. Electrochemical behavior of the MAWs in the composite during immersion: (a) Nyquist plots of the outer MAW after immersion for 4 days; (b) Nyquist plots of the inner MAW after 4 days; (c) Equivalent circuit model; (d) Evolution of R_p of MAWs in the composite versus immersion time.

Table 1
Molecular weight and bending strength retention of the samples under dynamic conditions after immersion for 21 days immersion.

Load parameter		M_v (10^4 g/mol)		S_b retention (%)	
Frequency	Magnitude	Pure PLA	Mg/PLA	Pure PLA	Mg/PLA
Static (no load)		4.31(±0.25)	5.32(±0.3)	82	83.3
0.5 Hz	0.9 MPa	3.61(±0.17)	4.29(±0.27)	72.7	76.3
1 Hz	0.1 MPa	3.77(±0.13)	4.46(±0.11)	74.5	72.3
	0.3 MPa	3.40(±0.14)	3.91(±0.03)	67.5	69.7
	0.9 MPa	3.19(±0.14)	3.66(±0.15)	60	66.1
2.5 Hz	0.9 MPa	2.73(±0.01)	3.34(±0.13)	50	60.1

decreases to 61% and 66% at static compression stress at 1 MPa, respectively [26]. The values are similar to those under dynamic loading at 1 Hz and 0.9 MPa after 21 days. A faster strength loss under the dynamic conditions indicates that dynamic loading accelerates implant failure in comparison with static loading. Moreover, increasing the stress level and frequency raises the degradation rate of pure PLA and Mg/PLA as reported previously [45] and therefore, the dynamic conditions should be considered in *in vitro* tests.

The implants are expected to decompose fully after fracture healing [46] but in practice, the implants may last for a long time up to 3 years or longer due to the slow degradation rate of PLA [47,48]. Since dynamic loading increases the degradation rate of PLA, dynamic loading at a large magnitude and large frequency can accelerate the process under physiological conditions, e.g. by doing exercise.

4.3. Degradation kinetics

Degradation of PLA is known to follow the first order kinetics during initial immersion [49,50]. The relationship between loga-

Table 2
Linearly fitted results for ln *Mv* and immersion time for pure PLA and Mg/PLA.

Load parameter		Pure PLA			Mg/PLA		
Frequency	Magnitude	A (g·mol^{-1})	k (g·mol^{-1}·day^{-1})	R^2	A (g·mol^{-1})	k (g·mol^{-1}·day^{-1})	R^2
static		11.19	0.017	0.98	11.21	0.015	0.99
0.5 Hz	0.9 MPa	11.19	0.034	0.99	11.19	0.025	0.99
1 Hz	0.1 MPa	11.23	0.03	0.91	11.21	0.023	0.97
	0.3 MPa	11.21	0.036	0.99	11.20	0.029	0.98
	0.9 MPa	11.18	0.04	0.98	11.18	0.033	0.99
2.5 Hz	0.9 MPa	11.18	0.047	0.99	11.18	0.033	0.99

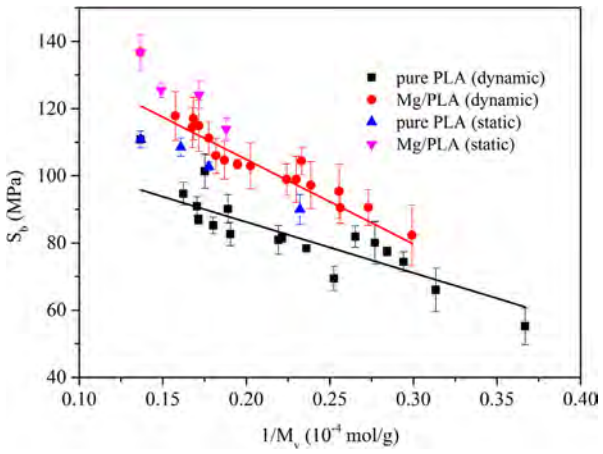

Fig. 8. Relationship between S_b and M_v in pure PLA and Mg/PLA.

Table 3
Fitted results of S_b and M_v for pure PLA and Mg/PLA.

	$S_{b\infty}$ (MPa)	B (MPa·g/mol)	R^2
Pure PLA	116.5	1.51 E6	0.67
Mg/PLA	155	2.52 E6	0.74

rithmic M_v of PLA and immersion time is expressed by the following equation and the fitted results are shown in Table 2:

$$\ln M_v = A - k \times t, \tag{2}$$

where A is a constant and k is the degradation rate. The good fit suggests that it is indeed first order. In addition, the initial degradation rates of the samples at 2.5 Hz, 0.9 MPa are 2 to 3 times those under static conditions furnishing evidence that dynamic loading accelerates initial degradation. It has been shown S_b and M_v for the pure PLA and the composite under static conditions have the following relationship [24,26,51,52]:

$$S_b = S_{b\infty} - B/M_v, \tag{3}$$

where $S_{b\infty}$ is the bending strength for a finite molecular weight and B is a constant. The fitted curves for pure PLA and Mg/PLA under dynamic conditions are shown in Fig. 8 and the fitted results are shown in Table 3. R^2 of pure PLA and Mg/PLA under dynamic conditions is only 0.67 and 0.74, indicating that the fitting according to Eq. (3) is not very good. Nonetheless, Eq. (3) can be applied to assess approximately the mechanical performance of the implants during dynamic immersion. Increased diffusion of acidic molecules out of the samples during dynamic loading may contribute to bending strength retention after a long period and it probably mitigates degradation of the inner MAWs and self-catalysis of PLA [53,54].

4.4. Degradation model

According to Eqs. (2) and (3), S_b exhibits the following relationship with immersion time (t):

$$S_b = S_{b\infty} - B/\exp(A - kt), \tag{4}$$

where k is obtained from the Arrhenius relationship:

$$k = k_0 \exp(-E_a/RT), \tag{5}$$

where k_0 is the pre-exponential factor, E_a is the activation energy, R is the gas constant, and T is the temperature. Under dynamic compression, degradation in a cycle involves two stages: static condition with no loading and compressive conditions. The relationship between k_0 and E_a obeys the compensation law [55] and this may explain why the external stress reduces k_0 and E_a simultaneously [56]. If E_a has a first-order relationship with the applied stress (σ) [57,58] and since the time in a cycle (s) is small compared to the immersion time (day), S_b for cycle i ($S_b(i)$) can be described by Taylor expansion as follows:

$$S_b(i) = \overbrace{S_b(i-1) + a'\left(\frac{1}{2f}\right) + b'\left(\frac{1}{2f}\right)^2}^{\text{Static condition with no load}} + a''\left(\frac{1}{2f}\right) + b''\left(\frac{1}{2f}\right)^2 + c'\sigma\left(\frac{1}{2f}\right) + d'\sigma\left(\frac{1}{2f}\right)^2 + e'\sigma^2\left(\frac{1}{2f}\right) + g'\sigma^2\left(\frac{1}{2f}\right)^2, \tag{6}$$

where a′, b′, a″, b″, c′, d′, e′ and g′ are constant and f is the frequency.

Then S_b can be described by the following model using a polynomial formula with seven constants:

$$S_b = \sum_0^{tf} S_b(i) = S_b(0) + at + b_t/f + c\sigma t + d\sigma t/f + e\sigma^2 t + g\sigma^2 t/f, \tag{6}$$

where $S_b(0)$, a, b, c, d, e, and g are constants. The fitted results under dynamic conditions are shown in Table 4 and Fig. 9 and the fitted and experimental results agree quite well.

Dynamic degradation tests are performed on the pure PLA and Mg/PLA composite at 2.5 Hz and 0.1 MPa for different immersion time (7, 10, 15, and 21 days) to verify the model. The experimental and calculated results in Fig. 10 are similar indicating that the model can describe the revolution of the bending strength under different dynamic conditions.

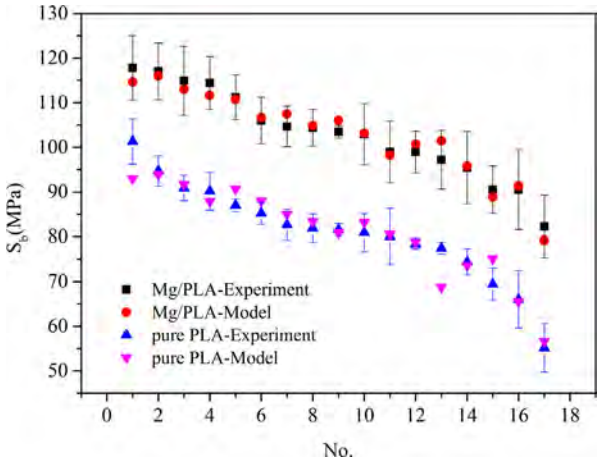

Fig. 9. Experimental and calculated results using the model for the bending strength under dynamic conditions.

Table 4
Fitted results using the model for bending strength under dynamic conditions.

	$S_b(0)$	a	b	c	d	e	g	R^2
Pure PLA	99.2	−0.59	0.133	−2.41	−0.76	0.55	1.56	0.82
Mg/PLA	121.6	−0.83	−0.024	−1.46	−0.0255	−0.22	1	0.93

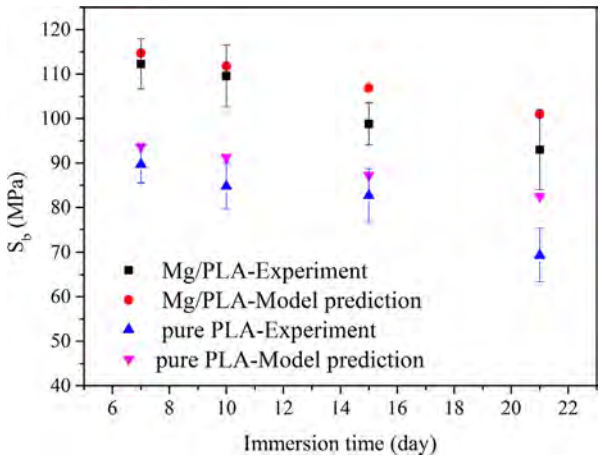

Fig. 10. Experimental data and calculated results based on the model for the bending strength of the pure PLA and Mg/PLA composite at 2.5 Hz and 0.1 MPa for different immersion time.

4.5. Advantages of the composite and the degradation model

An advantage of PLA-based biomaterials is their versatility and designability to be fabricated into a variety of required structures with appropriate mechanical and degradation properties for biomedical applications. However, the inadequate osteoconductivity still limits its further application in bone repair and fixation. Tricalcium phosphate (TCP) or hydroxyapatite (HA) is incorporated into PLA to enhance osteogenesis and prevent osteomyelitis [15]. Mg alloy based orthopedic implants has been shown to induce osteogenesis by promoting overexpression of calcitonin gene-related polypeptide-α (CGRP)-receptor-encoding genes Calcrl or Ramp1 [59]. A very recent study shows that the addition of Mg particle into PLA could significantly promote osteogenesis [20]. Moreover, it could be noticed Ca-P phase would precipitate on the surface of the MAWs in the composite especially under dynamic conditions at a large loading frequency which may enhance the diffusion of Ca and P through the interface between the MAWs and matrix. Thereby, the composite may also have great advantages on osteogenesis and biomineralization for bone repair and fixation.

Dynamic micromovement at the fracture gap can induce formation of calluses that bridge the fractured bones [6,7]. It is known that the healing process is highly sensitive to the degradation rate of the fixation material, which influences the bio-mechanical environment of the tissues surrounding the injured bones. *In vivo*, the mechanical properties of an ideal implant should match those of the surround tissues at each stage of the healing process. It should provide sufficient stabilization after surgical implantation followed by allowing gradual stress transfer to the fracture bones through material degradation. The proposed degradation model would provide a scientific basis for evaluating the mechanical adaptability in service and optimizing the structure of the implants. Moreover, with the corporation of mechano-regulation (MR) theories [60] which describe the relationship between tissue differentiation and the mechanical conditions, the best and most realistic loading conditions could be suggested for a particular composite implant to achieve successful healing bone fracture.

5. Conclusion

Dynamic compressive loading initially accelerates degradation of pure PLA and Mg/PLA and the degradation rate increases with the applied stress and frequency. The Mg/PLA composite delivers better mechanical performance under dynamic conditions. Initial degradation Mg/PLA comprises four stages and initial degradation of the pure PLA and PLA matrix in the composite under dynamic conditions obey the first order kinetics. The biomineralization would occur on the surface of MAWs in the composite under dynamic loading condition at a high loading frequency. A numerical model is proposed to describe the relationship of the bending stress, dynamic stress level, frequency, and immersion time and the calculated results and experiment data are in good agreement. The degradation model could be used for the determination of the loading conditions to achieve successful healing bone fracture.

Acknowledgements

This work was jointly supported by the National Natural Science Foundation of China (Grant No. 31570961, 51771054), State Key Program of National Natural Science Foundation of China (Grant No. 51631003), National Key Research and Development Program of China (Grant No. 2016YFC1102402), Hong Kong Research Grants Council General Research Funds No. CityU 11301215, and City University of Hong Kong Strategic Research Grant No. 7004644.

References

[1] N. Südkamp, J. Bayer, P. Hepp, C. Voigt, H. Oestern, M. Kääb, C. Luo, M. Plecko, K. Wendt, W. Köstler, Open reduction and internal fixation of proximal humeral fractures with use of the locking proximal humerus plate, J. Bone Joint Surg. Am. 91 (2009) 1320–1328.
[2] S. Perren, Physical and biological aspects of fracture healing with special reference to internal fixation, Clin. Orthop. Relat. Res. 138 (1979) 175–196.
[3] B. Hintermann, H. Trouillier, D. Schäfer, Rigid internal fixation of fractures of the proximal humerus in older patients, Bone Joint J. 82 (2000) 1107–1112.
[4] R. Schenk, H. Willenegger, Zum histologischen bild der sogenannten primärheilung der knochenkompakta nach experimentellen osteotomien am hund, Experientia 19 (1963) 593–595.
[5] D.A. Wiss, D.L. Johnson, M. Miao, Compression plating for non-union after failed external fixation of open tibial fractures, J. Bone Joint Surg. Am. 74 (1992) 1279.
[6] E.H. Schemitsch, A.F. Tencer, M.B. Henley, Biomechanical evaluation of methods of internal fixation of the distal humerus, J. Orthop. Trauma 8 (1994) 468–475.
[7] S. Olerud, G. Danckwardt-Lilliestrom, Fracture healing in compression osteosynthesis in the dog, Bone Joint J. 50 (1968) 844–851.
[8] G.N. Duda, F. Mandruzzato, M. Heller, J. Goldhahn, R. Moser, M. Hehli, L. Claes, N.P. Haas, Mechanical boundary conditions of fracture healing: borderline indications in the treatment of unreamed tibial nailing, J. Biomech. 34 (2001) 639–650.
[9] L. Claes, P. Augat, G. Suger, H.-J. Wilke, Influence of size and stability of the osteotomy gap on the success of fracture healing, J. Orth. Res. 15 (1997) 577–584.
[10] K. Bessho, T. Iizuka, K.-I. Murakami, A bioabsorbable poly-L-lactide miniplate and screw system for osteosynthesis in oral and maxillofacial surgery, J. Oral Maxillofac. Surg. 55 (1997) 941–945.
[11] Y. Shikinami, M. Okuno, Bioresorbable devices made of forged composites of hydroxyapatite (HA) particles and poly L-lactide (PLLA). Part II: Practical properties of miniscrews and miniplates, Biomaterials 22 (2001) 3197–3211.
[12] F.A. Barber, W.D. Dockery, Long-term absorption of poly-L-Lactic acid interference screws, Arthroscopy 22 (2006) 820–826.
[13] Y. Amano, M. Ota, K. Sekiguchi, Y. Shibukawa, S. Yamada, Evaluation of a poly-L-lactic acid membrane and membrane fixing pin for guided tissue regeneration on bone defects in dogs, Oral Surg. Oral Med. Oral Pathol. Oral Radiol. Endod. 97 (2004) 155–163.
[14] L. Janis, D.B. Kaplansky, W.T. DeCarbo, Early clinical experience with a fresh talar transplant inlay allograft for the treatment of osteochondral lesions of the talus, J. Am. Podiatr. Med. Assoc. 100 (2010) 25–34.
[15] G. Narayanan, V.N. Vernekar, E.L. Kuyinu, C.T. Laurencin, Poly (lactic acid)-based biomaterials for orthopaedic regenerative engineering, Adv. Drug Del. Rev. 107 (2016) 247–276.
[16] P. Nordström, T. Pohjonen, P. Törmälä, P. Rokkanen, Shear-load carrying capacity of cancellous bone after implantation of self-reinforced polyglycolic acid and poly-l-lactic acid pins: experimental study on rats, Biomaterials 22 (2001) 2557–2561.
[17] O. Böstman, J. Viljanen, S. Salminen, H. Pihlajamäki, Response of articular cartilage and subchondral bone to internal fixation devices made of poly-l-lactide: a histomorphometric and microradiographic study on rabbits, Biomaterials 21 (2000) 2553–2560.

[18] Y.F. Zheng, X.N. Gu, F. Witte, Biodegradable metals, Mater. Sci. Eng. R. 77 (2014) 1–34.
[19] A. Brown, S. Zaky, H. Ray, C. Sfeir, Porous magnesium/PLGA composite scaffolds for enhanced bone regeneration following tooth extraction, Acta Biomater. 11 (2015) 543–553.
[20] C. Zhao, H. Wu, J. Ni, S. Zhang, X. Zhang, Development of PLA/Mg composite for orthopedic implant: tunable degradation and enhanced mineralization, Compos. Sci. Technol. 147 (2017) 8–15.
[21] S.C. Cifuentes, R. Gavilán, M. Lieblich, R. Benavente, J.L. González-Carrasco, *In vitro* degradation of biodegradable polylactic acid/magnesium composites: Relevance of Mg particle shape, Acta Biomater. 32 (2016) 348–357.
[22] S.C. Cifuentes, E. Frutos, J.L. González-Carrasco, M. Muñoz, M. Multigner, J. Chao, R. Benavente, M. Lieblich, Novel PLLA/magnesium composite for orthopedic applications: a proof of concept, Mater. Lett. 74 (2012) 239–242.
[23] Y.H. Wu, N. Li, Y. Cheng, Y.F. Zheng, Y. Han, *In vitro* study on biodegradable AZ31 magnesium alloy fibers reinforced PLGA composite, J. Mater. Sci. Technol. 29 (2013) 545–550.
[24] X. Li, C. Chu, L. Zhou, J. Bai, C. Guo, F. Xue, P. Lin, P.K. Chu, Fully degradable PLA-based composite reinforced with 2D-braided Mg wires for orthopedic implants, Compos. Sci. Technol. 142 (2017) 180–188.
[25] X. Li, C. Guo, X. Liu, L. Liu, J. Bai, F. Xue, P. Lin, C. Chu, Impact behaviors of poly-lactic acid based biocomposite reinforced with unidirectional high-strength magnesium alloy wires, Prog. Nat. Sci-Mater. 24 (2014) 472–478.
[26] X. Li, C. Chu, Y. Wei, C. Qi, J. Bai, C. Guo, F. Xue, P. Lin, P.K. Chu, In vitro degradation kinetics of pure PLA and Mg/PLA composite: Effects of immersion temperature and compression stress, Acta Biomater. 48 (2017) 468–478.
[27] X. Li, C.L. Chu, L. Liu, X.K. Liu, J. Bai, C. Guo, F. Xue, P.H. Lin, P.K. Chu, Biodegradable poly-lactic acid based-composite reinforced unidirectionally with high-strength magnesium alloy wires, Biomaterials 49 (2015) 135–144.
[28] T.M. Skerry, Mechanical loading and bone: What sort of exercise is beneficial to the skeleton?, Bone 20 (1997) 179–181
[29] L.E. Lanyon, Using functional loading to influence bone mass and architecture: objectives, mechanisms, and relationship with estrogen of the mechanically adaptive process in bone, Bone 18 (1996) S37–S43.
[30] A.G. Robling, F.M. Hinant, D.B. Burr, C.H. Turner, Improved bone structure and strength after long-term mechanical loading is greatest if loading is separated into short bouts, J. Bone Miner. Res. 17 (2002) 1545–1554.
[31] C.H. Turner, M.R. Forwood, M.W. Otter, Mechanotransduction in bone: Do bone cells act as sensors of fluid flow?, FASEB J 8 (1994) 875–878.
[32] Y.-F. Hsieh, C.H. Turner, Effects of loading frequency on mechanically induced bone formation, J. Bone Miner. Res. 16 (2001) 918–924.
[33] C.L. Chu, X. Han, J. Bai, F. Xue, P.K. Chu, Fabrication and degradation behavior of micro-arc oxidized biomedical magnesium alloy wires, Surf. Coat. Technol. 213 (2012) 307–312.
[34] N.T. Kirkland, N. Birbilis, Magnesium biomaterials: Design, testing, and best practice, Springer, Switzerland, 2014.
[35] L.E. Lanyon, W.G. Hampson, A.E. Goodship, J.S. Shah, Bone deformation recorded in vivo from strain gauges attached to the human tibial shaft, Acta Orthop. 46 (1975) 256–268.
[36] A.H. Gruber, K.A. Boyer, T.R. Derrick, J. Hamill, Impact shock frequency components and attenuation in rearfoot and forefoot running, J. Sport Health Sci. 3 (2014) 113–121.
[37] L.E. Claes, C.A. Heigele, C. Neidlinger-Wilke, D. Kaspar, W. Seidl, K.J. Margevicius, P. Augat, Effects of mechanical factors on the fracture healing process, Clin. Orthop. Relat. Res. 355 (1998) S132–S147.
[38] A. Schindler, D. Harper, Polylactide. II. Viscosity–molecular weight relationships and unperturbed chain dimensions, J. Polym. Sci. Pol. Phys. Ed. 17 (1979) 2593–2599.
[39] K. Törne, A. Örnberg, J. Weissenrieder, Influence of strain on the corrosion of magnesium alloys and zinc in physiological environments, Acta Biomater. 48 (2017) 541–550.
[40] P. Wan, C. Yuan, L. Tan, Q. Li, K. Yang, Fabrication and evaluation of bioresorbable PLLA/magnesium and PLLA/magnesium fluoride hybrid composites for orthopedic implants, Compos. Sci. Technol. 98 (2014) 36–43.
[41] Y. Zhang, S. Zale, L. Sawyer, H. Bernstein, Effects of metal salts on poly(DL-lactide-co-glycolide) polymer hydrolysis, J. Biomed. Mater. Res. 34 (1997) 531–538.
[42] H. Mobedi, M. Nekoomanesh, H. Orafaei, H. Mivehchi, Studying the degradation of poly(L-lactide) in presence of magnesium hydroxide, Iran. Polym. J. 15 (2006) 31–39.
[43] D.E. Thompson, C.M. Agrawal, K. Athanasiou, The effects of dynamic compressive loading on biodegradable implants of 50–50% polylactic acid-polyglycolic acid, Tissue Eng. 2 (1996) 61–74.
[44] Y.-B. Fan, P. Li, L. Zeng, X.-J. Huang, Effects of mechanical load on the degradation of poly(d, l-lactic acid) foam, Polym. Degrad. Stab. 93 (2008) 677–683.
[45] G.D. Nicodemus, K.A. Shiplet, S.R. Kaltz, S.J. Bryant, Dynamic compressive loading influences degradation behavior of PEG-PLA hydrogels, Biotechnol. Bioeng. 102 (2009) 948–959.
[46] O. Böstman, H. Pihlajamäki, Clinical biocompatibility of biodegradable orthopaedic implants for internal fixation: a review, Biomaterials 21 (2000) 2615–2621.
[47] H. Tsuji, A. Mizuno, Y. Ikada, Properties and morphology of poly(L-lactide). III. Effects of initial crystallinity on long-term in vitro hydrolysis of high molecular weight poly(L-lactide) film in phosphate-buffered solution, J. Appl. Polym. Sci. 77 (2000) 1452–1464.
[48] R. Suuronen, T. Pohjonen, J. Hietanen, C. Lindqvist, A 5-year in vitro and in vivo study of the biodegradation of polylactide plates, J. Oral Maxillofac. Surg. 56 (1998) 604–614.
[49] V. Piemonte, F. Gironi, Kinetics of hydrolytic degradation of PLA, J. Polym. Environ. 21 (2013) 313–318.
[50] F. Codari, S. Lazzari, M. Soos, G. Storti, M. Morbidelli, D. Moscatelli, Kinetics of the hydrolytic degradation of poly(lactic acid), Polym. Degrad. Stab. 97 (2012) 2460–2466.
[51] I.M. Ward, J. Sweeney, Mechanical properties of solid polymers, John Wiley & Sons, New York, 2012.
[52] M. Deng, J. Zhou, G. Chen, D. Burkley, Y. Xu, D. Jamiolkowski, T. Barbolt, Effect of load and temperature on in vitro degradation of poly(glycolide-co-L-lactide) multifilament braids, Biomaterials 26 (2005) 4327–4336.
[53] Y. Shikinami, M. Okuno, Bioresorbable devices made of forged composites of hydroxyapatite (HA) particles and poly-L-lactide (PLLA): Part I Basic characteristics, Biomaterials 20 (1999) 859–877.
[54] G.L. Siparsky, Degradation kinetics of poly (hydroxy) acids: PLA and PCL, ACS Publications, Washington DC, 2000.
[55] Z. Huang, Q.-Q. Ye, L.-J. Teng, A comparison study on thermal decomposition behavior of poly(l-lactide) with different kinetic models, J. Therm. Anal. Calorim. 119 (2014) 2015–2027.
[56] N.Y. Rapoport, E.Z. Gennadii, Kinetics and mechanism of the oxidation of polymers in a stressed state, Russ. Chem. Rev. 52 (1983) 897–916.
[57] D.A. Davis, A. Hamilton, J. Yang, L.D. Cremar, D. Van Gough, S.L. Potisek, M.T. Ong, P.V. Braun, T.J. Martinez, S.R. White, J.S. Moore, N.R. Sottos, Force-induced activation of covalent bonds in mechanoresponsive polymeric materials, Nature 459 (2009) 68–72.
[58] M.K. Beyer, H. Clausen-Schaumann, Mechanochemistry: The mechanical activation of covalent bonds, Chem. Rev. 105 (2005) 2921–2948.
[59] Y. Zhang, J. Xu, Y.C. Ruan, M.K. Yu, M. O'Laughlin, H. Wise, D. Xhen, L. Tian, D. Shi, J. Wang, S. Chen, J.Q. Feng, D.H.K. Chow, X. Xie, L. Zheng, L. Huang, S. Huang, K. Leung, N. Lu, L. Zhao, H. Li, D. Zhao, X. Guo, K. Chan, F. Witte, H.C. Chan, Y. Zheng, L. Qin, Implant-derived magnesium induces local neuronal production of CGRP to improve bone-fracture healing in rats, Nat. Med. 22 (2016) 1160–1169.
[60] H. Mehboob, S.-H. Chang, Application of composites to orthopedic prostheses for effective bone healing: A review, Compos. Struct. 118 (2014) 328–341.